Available online at www.pelagiaresearchlibrary.com

Pelagia Research Library

Advances in Applied Science Research, 2010, 1 (1): 19-25

Steady-state and Transient Electron Transport Within Bulk III-V Nitride Semiconductors Using an Updated Semiclassical Three-valley Monte Carlo Method

H. Arabshahi*, M. Rezaee Rokn-Abadi, F. Badieyan and Z. Eslami Moghadam

Department of Physics, Ferdowsi University of Mashhad, Mashhad, Iran

---

ABSTRACT

An ensemble Monte Carlo simulation is used to compare high field electron transport in bulk InN, AlN and GaN. For all materials, we find that electron velocity overshoot only occurs when the electric field in increased to a value above a certain critical field .This critical field is strongly dependent on the material parameters. Transient velocity overshoot has also been simulated, with the sudden application of fields up to1000 kV/m , appropriate to the gate-drain fields expected within an operational field effect transistor. The electron drift velocity relaxes to the saturation value of 10^5 m/s within 3 ps, for all crystal structures. The steady state and transient velocity overshoot characteristics are in fair agreement with other recent calculations.

Keywords: *Velocity overshoot, gate-drain, transient, critical field, drift velocity.*

INTRODUCTION

GaN, and its related ternary compounds involving Al and In, have received much attention over the past years because of several new applications, including blue light-emitting diodes (LEDs), blue laser diodes (LDs) [1], and high-power microwave transistors [2-3]. However, one of the biggest problems to overcome has been the lack of a lattice-matched substrate, since bulk group III nitride semiconductors are very difficult to grow in large sizes [4-5]. The large band gap energy of the III-nitrides insures that the breakdown electric field strength of these materials is much larger than that of either Si or GaAs [6-7], enabling, at least in principle, much higher maximum output power delivery in power transistores. Additionally, it has been found that at least the binary compounds, GaN and InN, have higher electron saturation drift velocities and lower dielectric constants that can lead to higher frequency performance of devices made from these materials [8-9].

The fact that GaN, AlN and InN, can form type I heterojunctions with their related ternaries provides an additional advantageous quality for device design. Type I heterojunctions enable modulation doping techniques and their exploition in MODFET devices. In addition, the lattice mismatch between GaN and the ternary compound AlGaN in appropriately designed structures produces strain induced polarization fields [10-11]. These strain induced polarization fields can alter the band bending and carrier concentration at the heterointerface. In this way, the free carrier concentration can be increased within the channel region of a heterojunction field effect transistor, beyond that achievable by modulation doping alone.

For the above stated reasons, the III-nitride materials are of great interest for power FET and optoelectronic device structures. To clarify the expected performance of these materials, transport as well as device studies are critical. Thus, it is the purpose of this paper to compare steady state and transient velocity overshoot in binary group III-nitride using an ensemble Monte Carlo studies. This paper is organized as follows.
Details of the employed simulation model is presented in section 2 and the results of steady state and transient electron transport properties carried out on GaN, AlN and InN structures are interpreted in section 3.

Simulation model

In order to calculate the electron drift velocity for large electric fields, consideration of conduction band satellite valleys is necessary. The first-principles band structure calculation of Kim and Lambrecht [12] for wurtzite phase group III nitrides predict a direct band gap located at the Γ point and lowest energy conduction band satellite valleys at the U point (located two-thirds of the way between the L and M points) and at the K point. In our Monte Carlo simulation, the Γ valley, the two equivalent K valleys, and the six equivalent U valleys were represented by spherical, non-parabolic, analytical effective mass expressions of the following form [13-14],

$$\varepsilon(1+\alpha\varepsilon) = \frac{\hbar^2 k^2}{2m^*} \qquad (1)$$

The low energy effective masses, m^*, and the non-parabolicity factors, α, were obtained by matching equation 1 to the first principles bands [15]. The band structure and material parameters necessary for calculating the scattering probabilities used in the present Monte Carlo simulation are given in table 1. Scattering mechanisms included in the simulation are acoustic deformation potential, pizoelectric and ionized impurity scattering. Elastic ionized impurity scattering is described using the screened Coulomb potential of the Brooks-Herring model. Furthermore, longitudinal optical phonon scattering, nonequivalent and, where applicable, equivalent intervalley scattering events are taken into account among all valley types with the transfers assumed to be governed by the same deformation potential fields and the same phonon frequencies. Degeneracy effects are expected to be negligible over almost all of the temperature and electron concentration ranges of interest here and, hence, are not considered in the calculation. Electron particles in the ensemble Monte Carlo simulation occupy non-parabolic ellipsoidal valleys in reciprocal space, and obey Boltzmann statistics. Herring-vogt transformations are used to

map carrier momenta into spherical valleys when particles are drifted or scattered. The electric field equations are solved self-consistently with the electron transport using a finite difference method [16-18], and the device grid potentials are updated at each ensemble drift timestep (1 femtosecond).

Table 1: Valley and material parameters of energy band structure for wurtzite structure of InN, AlN and GaN used in the present Monte Carlo simulation [19-21]

	GaN	InN	AlN
Density ρ (kgm^{-3})	6150	6810	3230
Longitudinal sound velocity v_s (ms^{-1})	6560	6240	9060
Low-frequency dielectric constant ε_s	9.5	15.3	8.5
High-frequency dielectric constant ε_∞	5.35	8.4	4.77
Acoustic deformation potential (eV)	8.3	7.1	9.5
Polar optical phonon energy (eV)	0.0995	0.089	0.0992
Γ-valley effective mass (m^*)	0.2	0.11	0.31
U-valley effective mass (m^*)	0.4	0.4	0.39
K–valley effective mass (m^*)	0.3	0.3	0.56
Γ-valley nonparabolicity (eV^{-1})	0.189	0.419	0.32
U-valley nonparabolicity (eV^{-1})	0.065	0.065	0.5
K-valley nonparabolicity (eV^{-1})	0.7	0.7	0.03

RESULTS AND DISCUSSION

The bulk group-III nitride velocity-field characteristics, predicted by our model are shown in figure 1. For all cases, the temperature is 300 K and the donor concentration is 10^{22} m^{-3}. We see that each compound exhibits a peak in its velocity-field characteristic.

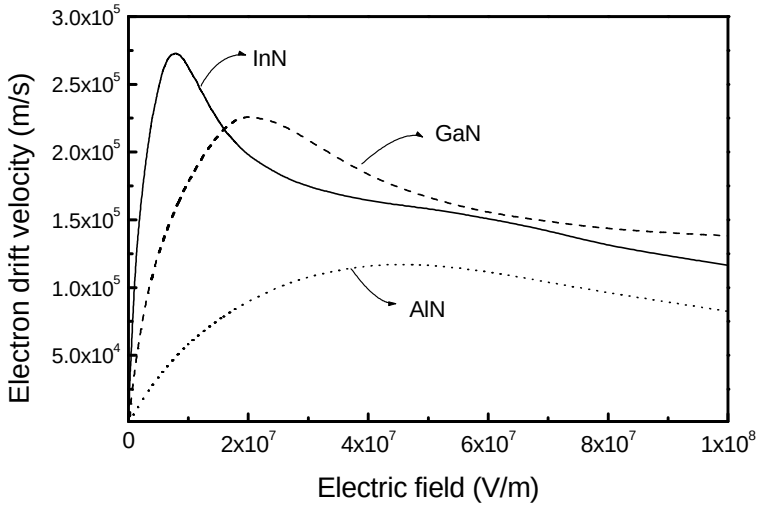

Fig 1: Calculated electron drift velocity in AlN, GaN and InN as function of applied electric field at room temperature

The peak drift velocity for InN is around $2.7\times10^5\,ms^{-1}$ while those for GaN and AlN are about $2.26\times10^5\,ms^{-1}$ and $1.2\times10^5\,ms^{-1}$, respectively. At higher electric fields the drift velocity decreases, eventually saturating at around $1.5\times10^5\,ms^{-1}$ and $8\times10^4\,ms^{-1}$ for GaN, InN and AlN, respectively.

The calculated drift velocities apparent from figure 1 are fractionally lower than those that have been calculated by Bellotti et al. [22], who assumed an effective mass in the upper valleys equal to the free electron mass. The threshold field for the onset of significant scattering into satellite conduction band valleys is a function of the intervalley separation and the density of electronic states in the satellite valleys.

The valley occupancies for the Γ, U and K valleys are illustrated in figure 2 and show that the inclusion of the satellite valleys in the simulation is important. Significant intervalley scattering into the satellite valleys occurs for fields above the threshold field for each material. This is important because electrons which are near a valley minimum have small kinetic energies and are therefore strongly scattered. It is apparent that intervalley transfer is substantially larger in InN over the range of applied electric fields shown, due to the combined effect of a lower Γ effective mass, lower satellite valley separation energy, and slightly lower phonon scattering rate within the Γ -valley.

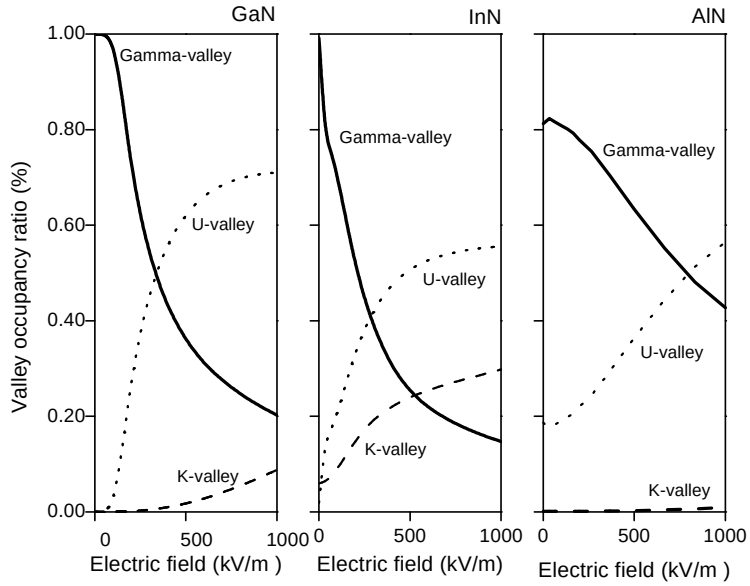

Fig 2: Comparison of the valley occupancies as function of electric field in bulk wurtzite InN, GaN and AlN structures at room temperature

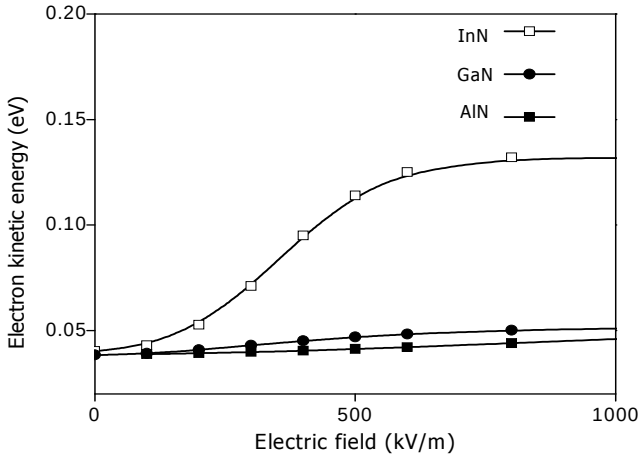

Fig 3: Average electron kinetic energy as a function of applied electric field in bulk wurtzite InN, GaN and AlN structures at room temperature

The average carrier kinetic energy as a function of electric field is shown in figure 3. The curves have the S shape typical of III-V compounds, which is a consequence of intervalley transfer. At high fields, the curve for InN suggests that the average electron energy is higher than for AlN and GaN. This difference can be understood by considering the Γ-valley occupancy as a function of field (figure 2). Intervalley transfer is substantially larger in the InN than AlN or GaN, due to the combined effect of a lower Γ -valley effective mass, lower satellite valley separation and reduced phonon scattering rate within the Γ-valley, but significant intervalley phonon scattering at a threshold field of 500kVm^{-1}.

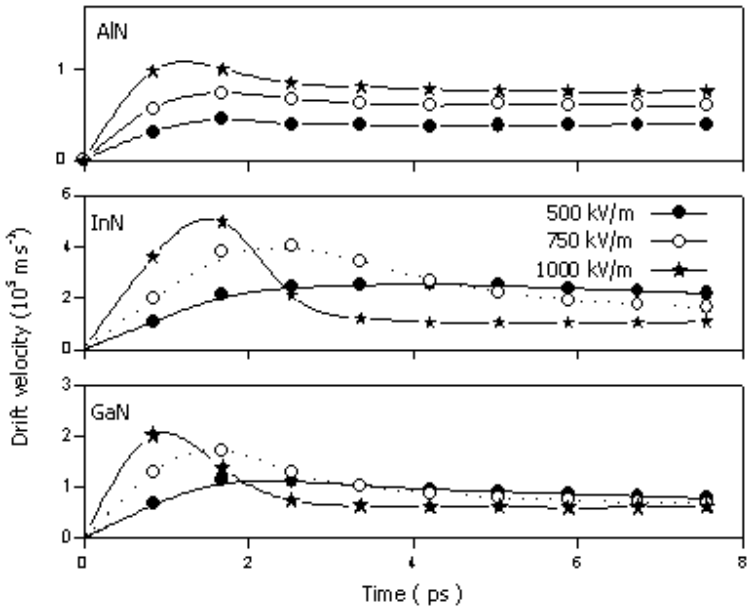

Fig 4: A comparison of the velocity overshoot effect exhibited by the AlN, InN and GaN semiconductors as calculated by our Monte Carlo simulation. The donor concentration is 10^{22} m^{-3} and the temperature is 300 K

We have also examined transient electron transport in bulk AlN, GaN and InN. The transient response of electrons in these materials are compared in figure 4 for different electric field strengths. Note that the overshoot velocity in InN is higher and is more enduring than for the other materials. When the field is increased to 1000 kVm^{-1} the peak velocity in InN increases to 4.5×10^{5} ms^{-1}. The velocity overshoot effect in AlN is markedly weaker. This is because of the smaller intervalley energy separation, 0.61 eV (versus 1.9 eV in GaN and 2 eV in InN) and larger Γ effective mass, 0.31 m_0 (versus 0.2 m_0 in GaN and 0.11 m_0 in InN). The smaller satellite energy separation means that the electrons readily transfer to the satellite valleys, resulting in a reduced average electron velocity and the rapid removal of overshoot.

CONCLUSION

The computed steady-state and transient electron transport in wurtzite GaN, AlN and InN show that InN has superior electron transport properties. The velocity-field characteristics of the materials show similar trends, reflecting the fact that these semiconductors have satellite valley effective densities of states several times greater than the central *Γ*-valley. We have also shown that GaN exhibits much more pronounced overshoot effects compared to AlN but at much higher electric fields. Using valley models to described the electronic band structure, it is found that electron drift velocity relaxes to the saturation value within 3 ps in GaN, AlN and InN crystal structures.

Acknowledgments

I would like to thank the partial support of this work by the Ferdowsi University of Mashhad.

REFERENCES

[1] S Nakamura, M Senoh and T Mukai, *Appl. Phys. Lett*. **1993,** 62, 2390
[2] S Strite and H Morkoc, *J. Vac. Sci. Technol. B* **1992**, 10, 1237
[3] R. J. Trew, M. V. Shin and V. Gatto, *Solid state Electron*. **1997,** 41, 1561
[4] V W L Chin and T L Tansley, *J. Appl. Phys.* **1994**, 75, 7365
[5] D L Rode and D K Gaskill, *Appl. Phys. Lett.* **1995**, 66, 1972
[6] H Brooks, *Phys. Rev.B.* **1951,** 83, 879
[7] J R Meyer and F J Bartoli, *Phys. Rev. B* **1981**, 23, 5413
[8] J R Meyer and F J Bartoli , *Solid State State Commun.* **1982**, 41, 19
[9] C Erginsoy, *Phys. Rev*. **1950**, 79, 1013
[10] C Schwartz, *Phys. Rev.* **1961**, 124, 1468
[11] M V Fischetti, *Phys. Rev.* **1991**, 44, 5527
[12] W. R. L. Lambrecht, *III-Nitrides*, Academic, New York, **1996**
[13] C Moglestue, *Monte Carlo simulation of semiconductor devices*, Chapman and Hall **1993**
[14] B K Ridley, *Electrons and phonons in semiconductor multilayers*, Cambridge University
[15] C Erginsoy, *Phys. Rev*. **1950,** 79, 1013

[16] C Schwartz, *Phys. Rev.* **1961**, 124, 1468
[17] M V Fischetti, *Phys. Rev.* **1991**, 44, 5527
[18] H Morkoc, *Nitride semiconductor and devices*, Springer-velag **1999**
[19] Udayan, V Bhapkar and M S Shur, *J. Appl. Phys.* **1997**, 82, 1649
[20] R P Wang, P P Ruden, J Kolnik and K F Brennan, *Mat. Res. Soc. Symp. Proc*., 445, 935
[21] H Morkoc, *Nitride semiconductor and devices*, Springer-velag **1999**
[22] E. Bellotti, B. K. Doshi and K. F. Brennan, *J. Appl. Phys.*, **1999**, 85, 916